Ann. For. Sci. 63 (2006) 43–53
© INRA, EDP Sciences, 2006
DOI: 10.1051/forest:2005096

Original article

The angular distribution of diffuse photosynthetically active radiation under different sky conditions in the open and within deciduous and conifer forest stands of Quebec and British Columbia, Canada

Fidji GENDRON[a,b]*, Christian MESSIER[a], Ernest LO[a], Philip G. COMEAU[c]

[a] Groupe de recherche en écologie forestière interuniversitaire (GREFi), Département des sciences biologiques, Université du Québec à Montréal, case postale 8888, succursale Centre-Ville, Montréal, QC H3C 3P8, Canada
[b] Current address: Luther College, University of Regina, Regina, Saskatchewan, S4S 0A2, Canada
[c] Department of Renewable Resources, University of Alberta, Faculty of Agriculture, Forestry and Home Economics, University of Alberta, 442 Earth Sciences Building, Edmonton, Alberta T6G 2E3, Canada

(Received 17 December 2004; accepted 24 August 2005)

Abstract – The angular distribution of diffuse photosynthetically active radiation (PAR) was characterised in the open and beneath deciduous and conifer forests in Quebec and British Columbia, Canada, under overcast and clear sky conditions, using a restricted field of view light sensor and hemispherical canopy photographs. The angular distribution of PAR was described by the relative light reading (RLR). In the open on overcast days, light was best characterized using the standard overcast sky distribution with the light intensity at the zenith set to four to five times greater than the light intensity at the horizon. RLR under forest stands was found to decrease with decreasing elevation angles under both overcast and clear sky conditions. Aspen (*Populus tremuloides* Michx.) and Jack pine (*Pinus banksiana* Lamb.) stands transmitted more light from a relatively wider angle around the zenith than the spruce (*Picea glauca* (Moench) Voss and *Picea mariana* (Mill.) BSP) stands, which transmitted light mainly from the zenith. RLR estimated with the hemispherical canopy photographs (RLR_{hc_corr}) generally provided a comparable prediction of the effect of the canopy composition on the angular distribution of PAR.

coniferous forest / deciduous forest / diffuse radiation / photosynthetically active radiation

Résumé – Distribution de la radiation photosynthétiquement active sous différentes conditions de ciel en milieu ouvert et sous peuplements forestiers de feuillus et de conifères au Québec et en Colombie-Britannique, Canada. La distribution angulaire de la radiation photosynthétiquement active (PAR) a été mesurée en milieu ouvert et sous peuplements de feuillus et de conifères situés au Québec et en Colombie-Britannique lors de journées nuageuses et ensoleillées à l'aide d'un senseur à angle restreint et de photographies hémisphériques. La distribution angulaire du PAR a été estimée par une lecture de lumière relative (LLR). En milieu ouvert lors de journées nuageuses, LLR déclinait du zénith vers l'horizon, avec des mesures au zénith de quatre à cinq fois plus élevées qu'à l'horizon. LLR mesurée sous couvert forestier déclinait du zénith vers l'horizon lors de journées nuageuses et ensoleillées. Les peuplements de peupliers (*Populus tremuloides* Michx.) et de pins gris (*Pinus banksiana* Lamb.) ont transmis relativement plus de PAR sous un angle plus large autour du zénith que les peuplements d'épinettes (*Picea glauca* (Moench) Voss et *Picea mariana* (Mill.) BSP) qui ont principalement transmis du PAR autour du zénith. La distribution angulaire du PAR estimée avec les LLR mesurées avec la photographie hémisphérique sous les différents couverts forestiers correspondait de façon générale aux résultats obtenus avec le senseur.

forêt de conifères / forêt feuillue / rayonnement diffus / rayonnement photosynthétiquement actif

1. INTRODUCTION

There have been very few studies on how understory light is distributed over elevation and azimuth angles, and on the influence of forest species composition in determining this angular distribution. The angular distribution of diffuse PAR in the understory may be an important factor in shaping crown morphology and in influencing light interception from the understory vegetation layers. For example, the crowns of four tropical deciduous tree species have been found to be oriented toward the direction of maximum diffuse light penetration [1]. Similarly, leaves of the understory juvenile tree *Pseudopanax crassifolius* were oriented toward the largest gaps presumably in order to increase diffuse light interception [13]. Crowns of *Pinus sylvestris* were oriented toward southerly directions, the directions with the greatest incoming solar radiation, when the light availability was not reduced by local competition [34]. The aim of this study is to characterize the angular distribution of PAR in both open and forest understory conditions, for clear and overcast skies, and over a range of sites using light sensor measurements and hemispherical photographs. This study is limited in scope to the characterization of the diffuse component

* Corresponding author: fidji.gendron@uregina.ca

of PAR only. In addition, the most common method of measuring the angular distribution of PAR, that of hemispherical photography, is evaluated by comparison to reference measurements made with the light sensor.

The first objective in this study is to characterize the above-canopy diffuse light distribution for the study sites. There have been many studies of the open-sky diffuse light distribution, and most have characterized the light distribution across the sky in open conditions, for overcast skies [5, 21, 28, 41]. There is an ongoing debate, however, as to the precise form of the above-canopy diffuse light distribution, with most of the debate centered on the well-known standard overcast sky (SOC) and universal overcast sky (UOC) models. The SOC model predicts that the diffuse light intensity is highest at the zenith and decreases toward the horizon [5, 28]. This contrasts with the isotropic and uniform sky light distribution found in the UOC [7, 8]. The SOC formula was initially developed by Moon and Spencer [28]. They suggested that the zenith-to-horizon radiance ratio ($1 + b$) should equal 3, making the zenith three times brighter than the horizon. In studies on global radiation (300–3000 nm), the b parameter has been found to vary greatly (from 1 to 5) according to the wavelengths measured, the cloud density, and the cloud height [21, 41], with the mean and modal value occurring at 1.23 [5]. In the few studies that have characterized the PAR band (400–700 nm), the decrease in brightness from the zenith to the horizon was equally variable, with the b parameter ranging from 2 to almost 5 [19, 21]. In general the open-sky diffuse light distribution (as characterized by overcast skies) seems to vary with angle, with its exact functional form being site-dependent.

The diffuse sky brightness also includes a contribution from clear skies. The clear sky diffuse light distribution is not well known and is neglected in most studies and light models. It can be measured by detecting the angular distribution of radiance during clear conditions, from all directions except the position of the solar disc. In this study both the overcast and clear-sky diffuse light distributions were characterized over different study sites, and the suitability of the SOC and UOC equations to represent these distributions was assessed.

The second objective of this study was to characterize the angular distribution of diffuse PAR in stands of aspen (*Populus tremuloides* Michx.), Jack pine (*Pinus banksiana* Lamb.) and spruce (*Picea glauca* (Moench) Voss and *Picea mariana* (Mill.) BSP) in Quebec, and stands of red alder (*Alnus rubra* Bong.) and Douglas-fir (*Pseudotsuga menziesii* (Mirb.) Franco) in British Columbia, Canada. The understory PAR distribution is determined by the attenuation of the above-canopy light by foliage and branches and, therefore, is expected to depend on and to reflect the forest canopy structure. The effect of forest stands on total light transmission [25, 26], spectral changes [33] and total light variability [18] have been well-documented in the literature. However, few studies have explored the variation of the understory light as a function of elevation and azimuth angles (i.e. the angular distribution of PAR), and how this distribution might be influenced by the forest species composition. For example, although the light beneath forest canopies is generally believed to originate mainly from directly overhead [29, 38, 39], some studies also report that lateral light coming from mid to low elevation angles represent a sizable component of total light that reaches understory plants [12, 13]. Characteristics of forest stands that might influence the variation in angular distribution of PAR include: crown shape, branch and leaf distribution and orientation within the canopy, leaf area density within the canopy and the degree of overlap which occurs between the individual trees that comprise a stand. As these characteristics vary with the species composition of the canopy, the understory PAR distribution is expected to be a function of forest species composition as well.

With few exceptions [20, 43], the angular distribution of PAR beneath plant canopies has been estimated with the hemispherical canopy photograph technique [7–9, 22, 30]. However, photographic analysis only considers light that penetrates directly through openings in the canopy and does not take into account light transmission and reflection by vegetation, the penumbra effect and the detailed and uneven distribution of diffuse light brightness [8, 10, 44]. A restricted field of view light sensor, however, is capable of measuring the total (i.e. all contributions from vegetation scattering or transmission) quantity of light received in the understory as a function of angle [19, 20]. Few other studies have used such a light sensor [19, 20], however, mainly because its implementation is time-consuming, which limits the number of microsites that can be sampled. For the third objective of this study, the light sensor is used as a reference against which the accuracy of the hemispherical photograph method is compared and evaluated, in the context of measuring the angular distribution of diffuse PAR.

2. MATERIALS AND METHODS

2.1. Study sites

The study sites were located at the Duparquet Lake Research Station in Quebec and on Vancouver Island in British Columbia, Canada. Forest stands at the Duparquet Lake Research Station (48° 30' N, 79° 20' W) originated from a 1923 fire and were characterised by mature stands of aspen, Jack pine, and spruce. One of the spruce stands originated from a 1760 fire. The Quebec stands were all located on clay soils. Forest stands on Vancouver Island were located in a 89-year-old Douglas-fir stand and a 45-year-old red alder stand. The Douglas-fir stand was located near Cowichan Lake on southern Vancouver Island, British Columbia (48° 49' N, 124° 07' W). This forest stand originated from a 1909 fire and the soils were Humo-ferric Podzols and of sandy loam texture [42]. The canopy was uniform with a subcanopy of western hemlock (*Tsuga heterophylla* (Raf.) Sarg.) and western redcedar (*Thuja plicata* Donn ex D. Don). The red alder stand was located close to Sarita Lake (48° 55' N, 124° 54' W), approximately 90 km north-west of Cowichan Lake. Sitka spruce (*Picea sitchensis* (Bong.) Carr.) was present in the subcanopy.

Five circular, 11.28 m radius plots were installed in each stand for measurement purposes with the Douglas-fir stand being large enough to contain six plots. A visual assessment of the canopy was made before installing each plot to ensure that there was no slope and that the canopy was uniform, closed, and composed predominantly (more than 80%) of the desired canopy species. There was at least 20 m of similar habitat on all sides of the selected plots, and adjacent plots within a stand were separated by at least 20 m. The separation distance between each plot minimized redundant measurement of the same trees for different plots. The center of each plot was located at least 2 m from the closest stem in the middle of a group of trees. Since the objective of the study was to examine the effect of the forest canopy on the angular distribution of PAR, understory vegetation taller than 1 m

Table I. Stand characteristics. N/A: data not available.

Stand composition	Density (No./ha)	Height (m)	Live crown ratio (%)	Average DBH (cm)	Basal area ($m^2 \cdot ha^{-1}$)	Light (%)
Duparquet Lake Research Station, Quebec						
Aspen 1	1100	N/A	N/A	21	40	15.0
Aspen 2	1851	25	28	21	47	17.5
Aspen 3	775	27	23	22	32	19.5
Aspen 4	875	27	37	22	40	14.0
Aspen 5	1075	28	21	26	60	15.1
Jack pine 1	1276	25	42	19	40	16.3
Jack pine 2	1376	23	29	17	37	17.0
Jack pine 3	1075	22	18	19	34	15.9
Jack pine 4	1051	23	25	19	32	14.8
Jack pine 5	1026	23	31	20	34	12.2
Spruce 1	1701	18	63	16	36	6.9
Spruce 2	1751	17	50	17	42	8.2
Spruce 3	1526	17	56	16	31	10.1
Spruce 4	1501	16	57	17	38	10.9
Spruce 5	1951	19	N/A	15	37	5.1
Vancouver Island, British Columbia						
Red alder 647	951	23	29	24	47	11.1
Red alder 648	725	23	50	24	38	8.9
Red alder 649	1151	27	33	22	48	7.8
Red alder 650	1226	20	36	26	70	9.6
Red alder 2921	1226	25	15	23	57	11.5
Douglas fir 2876	1076	39	24	27	80	7.9
Douglas fir 2877	575	47	26	35	68	6.4
Douglas fir 2880	650	45	33	37	78	15.73
Douglas fir 2881	876	43	20	31	75	6.5
Douglas fir 2882	725	46	24	32	81	10.7
Douglas fir 2883	1201	48	30	33	101	7.3

was cut within each plot. This operation was required in the aspen, Jack pine and red alder plots. Understory vegetation in the spruce and Douglas-fir plots was minimal. Diameter at breast height and total tree height were recorded within each plot for representative trees (Tab. I). Stand age was estimated from tree ring counts taken from two average-sized trees within each plot and from fire age. The live crown ratio was calculated as the percentage of total tree height.

2.2. Technical information about the light sensor

The construction of the light sensor and the head is described in Fielder and Comeau [16] and Grace [19], respectively. The light sensor consisted of a gallium arsenide phosphide photodiode (Hamamatsu, model G1117, Middlesex, NJ, USA). Photodiodes are particularly useful for plant ecophysiological studies because they possess a very linear response to quantum flux over the 300 to 680 nm (i.e. PAR) range. The light sensors measured radiance as quanta per unit time per unit area from an area of sky subtending a 23.42° solid angle. The photodiode was glued onto the flat surface of a tubing of delrin rod which was then inserted into an aluminium tube. The photodiode was connected to a communication cable attached to a LI-COR datalogger (model LI-1000, LI-COR Inc., Lincoln, NE, USA) which measured the electrical current expressed in microAmps. The base of the sensor body was filled with Dow Corning RTV silicon sealant to ensure it was watertight. In order to restrict the viewing angle of the photodiode, a 23.42° field of view head was built and then placed on the top of the sensor body. The head consisted of a 62.34 mm long aluminium tube. Rings of delrin rod were placed inside the aluminium tubing to serve as baffles. Grace [19] reported that baffles were necessary as they decrease stray light by 10 to 15%. Matte black paint was applied to all the components in order to reduce light reflection inside the head. Two light sensors were built according to this design. The two sensors were calibrated twice in a large clearcut in July, and both sensors were found to be highly correlated (Spearman's rank correlation coefficient = 0.96). As the data presented in this study are based on relative light readings, the slight difference in sensitivity observed between the two sensors was unimportant.

2.3. Directional light measurements

Each light sensor was mounted on a separate 1.5 m tripod so that two users could make light measurements at the same time, in different plots. The sensor was glued to a black, 7.5 cm × 7.5 cm plexiglass plate that was firmly screwed to the top of a tripod. The light measurements were recorded at various angles by tilting and rotating the sensor. Light readings were made over eight elevation angles from 90º (the zenith) to 20º, at 10º increments, and over eight azimuth angles (N, NE, E, SE, S, SW, W, and NW). Note that elevation angle is defined in this study as being zero at the horizon and reaching 90 at the zenith. A tilt meter and a compass were used for setting the light sensor to the desired elevation and azimuth angles. The light sensor was connected to the LI-COR datalogger and the light readings were recorded instantaneously. A complete scan consisted of 64 readings and required less than 25 min. One complete scan was completed during each time period (described below) for each plot. For each scan, the relative light reading (RLR_{sensor}) was calculated as the light reading at elevation angle θ and azimuth angle γ, divided by the sum of light readings over the eight elevations and eight azimuth angles, multiplied by 100:

$$RLR_{sensor}(\theta,\gamma) = (\text{light reading}(\theta,\gamma) / (\text{sum of light readings over the eight elevation and eight azimuth angles}) \times 100. \quad (1)$$

In the present study, the angular distribution of PAR was described by the RLR_{sensor} profile. Due to the extremely high radiance of the sun, the current signal to the datalogger became saturated for the measurements when the sensor was pointing at the sun under clear sky conditions. Sensor saturation was one reason that light measurements in the present study were restricted to diffuse light only and that measurements at or near the solar angle were excluded.

To determine the effects of sky conditions on the angular distribution of PAR, light measurements were made during three time periods: (1) overcast sky conditions (between 10 h 00–14 h 00, solar time), (2) clear sky conditions in the morning (9 h 00–11 h 00), and (3) clear sky conditions around noon (11 h 00–13 h 00). Under overcast sky conditions, the sky was completely covered with clouds. On clear sky conditions, there was less than 20% cloud coverage, and also light measurements were done in a sequence that avoided pointing the sensor in the direction of any clouds. The light measurements were collected sufficiently quickly during these different periods so that the movement of the sun across the sky was negligible. One of the spruce plots was measured just once in the morning under clear sky conditions. Some of the data for clear sky conditions had to be eliminated when clouds were noted later during the scanning. All light measurements were completed under windless conditions. In addition to those light measurements recorded in the plots, the angular distribution of PAR was also measured in an open area using the same sampling procedure; one complete scan was made for each time period.

Measurements were made from July 11 to August 8 for the Duparquet Lake Research Station sites, except for those measurements made in the open, under overcast sky conditions, which were made on August 24. Light measurements were made from September 12 to October 1 for the Vancouver Island sites, and all of those in the red alder stand were done before September 20, before the leaves started to fall.

2.4. Modelling of the diffuse angular light distribution in open conditions

In this study, the angular distribution of PAR for open overcast skies is modelled using the well-known standard overcast sky distribution (SOC) [5, 28]. The SOC is the brightest at the zenith, with the light decreasing towards the horizon; it is uniform azimuthally.

$$\text{overcast sky } RLR_{sensor}(\theta) \propto (1 + b \cdot \sin(\theta)) / (1 + b). \quad (2)$$

Here we have used the fact that RLR is proportional to the radiance distribution, where the constant of proportionality is determined by the measured RLR at the zenith (i.e. RLR_{sensor} (90º)).

The term (1+ b) represents the ratio of radiance at the zenith to that at the horizon [41]. For example, when the zenith-to-horizon radiance ratio parameter (b) is set to 2 the zenith is three times brighter than the horizon, i.e. overcast sky RLR_{sensor} (0°)/RLR_{sensor}(90º) = 1/3. The b parameter has been found to vary from 1 to 5 [21, 41]. Consequently, the first step was to determine which value of b best described the sky angular distribution of PAR in the present study. With regards to the azimuthal uniformity, our data was found to be consistent with this assumption: overcast sky RLR_{sensor} did not vary with azimuth angle at the Duparquet Lake Research Station (one-way ANOVA, $F_{7,56}$ = 0.41, P = 0.8930). On Vancouver Island, overcast sky RLR_{sensor} showed some variation with azimuth angle (one-way ANOVA, $F_{7,54}$ = 2.67, P = 0.0191), but these differences were not related to the position of the sun (overcast sky RLR_{sensor} was highest in the NW direction and lowest in the SE direction). Note that in contrast to diffuse light, the angular distribution of direct light depends on the sun's trajectory across the sky over the growing season, and since this is well-described in [17], it was not investigated in this study.

2.5. Hemispherical canopy photographs

Hemispherical canopy photographs were taken using a Nikon FM2 camera equipped with a Sigma 8 mm fisheye lens. The camera was mounted with its top to the north, on a tripod 1.5 m in height above the forest floor, and installed at the same location as the light sensor. Photographs were taken early in the morning or at the end of the afternoon in order to optimize contrast and to minimize glare from direct sunlight [6, 14]. All photographs were underexposed to further increase contrast between sky and foliage. After processing, the negatives (Kodak TMAX 400 black and white film) were transferred onto a Kodak Photo CD master disc with a resolution of 768 × 512 pixels. Boundaries for the photos were determined with the Adobe Photoshop® program (version 5.0 for Windows®, Adobe Systems Inc., San Jose, CA, USA) by comparing them with photos taken in the open. Two small dots were placed at the outer east and west sides to mark the maximum diameter of the photos.

The hemispherical canopy photographs were analysed to calculate the transmitted light for different elevation and azimuth angles, using the Gap Light Analyzer (GLA) program [17]. GLA has been used extensively for such forest light calculations [7], ([8] a previous version, GLI/C, was used). Analysis of the photographs was performed as described in the users' manual [17]. As only the relative amount of diffuse light calculated from the GLA is considered in our study (one exception was the total % light in Tab. I), the beam fraction and clear sky transmission in the GLA model were unimportant. An SOC sky distribution model was used as an input parameter to describe the above-canopy light for the analysis. Photograph analysis was conducted for the period between July 11 and August 8 at the Duparquet Lake Research Station, and between September 12 and October 1 on Vancouver Island. In the analysis of the GLA results, the sky hemisphere was partitioned into 648 sky regions using 10° elevation divisions and 5° azimuth divisions. Some database work was then necessary to aggregate these sky regions in order to approximate the 23° solid angle of the light sensor. Twenty degrees increments in elevation were centred on the same eight elevation angles as the light sensor and averaged over azimuth angles.

TransDiffuse is the absolute ($mol \cdot m^{-2} \cdot d^{-1}$) amount of diffuse radiation found at an understory microsite over a growing season [17], and was calculated from the hemispherical photographs using the GLA. The relative light reading for the hemispherical canopy photographs (RLR_{hc}) is then determined from this quantity:

$$RLR_{hc}(\theta,\gamma) = (\text{TransDiffuse}(\theta,\gamma) / (\text{TransDiffuse over the eight elevation and eight azimuth angles}) \times 100. \quad (3)$$

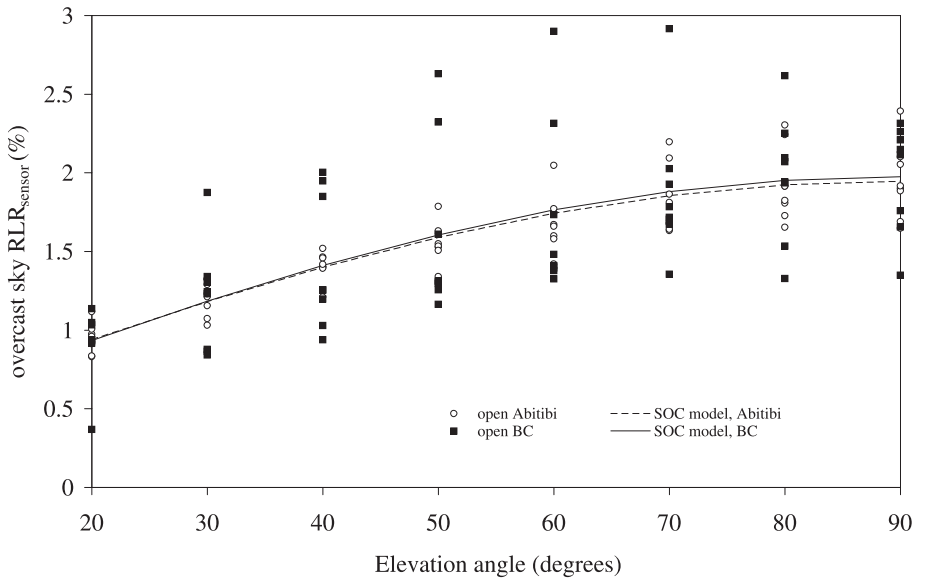

Figure 1. Relative light readings measured in the open under overcast sky conditions with the light sensor (overcast sky RLR_{sensor}) and modelled with the SOC sky distribution at the Duparquet Lake Research Station in Abitibi and on Vancouver Island in British Columbia.

In the calculations, the sky was partitioned by the GLA into discrete sky regions of 10° increments in elevation and 5° increments in azimuth. Percent (%) of light transmission was calculated by the GLA for the entire hemisphere, and ranged from 0%, when there were no gaps in the canopy (i.e. a closed canopy), to 100% for a site in the open ([6] a previous version, GLI/C, was used).

2.6. Correction of RLR_{hc}

RLR_{hc} is not directly comparable to the RLR_{sensor} for two reasons. Firstly, the light reading (i.e. TransDiffuse) calculated by the GLA scales uses the area of its sky region; this area varies with elevation angle, being smallest at the zenith and largest at the horizon. In contrast, sensor light measurements have a constant angular aperture of 23.45°. Secondly, TransDiffuse is calculated on the basis of the light flux incident on a horizontal surface, while light measured with the sensor represents the incident light flux normal to the propagation direction, referred to as a "ball-sensor measurement". Therefore, two correction factors have been introduced to RLR_{hc}, that normalize its TransDiffuse terms to the area of sky region and convert it to a normally incident light value. This corrected RLR_{hc} is termed RLR_{hc_corr} and is equivalent and comparable to the sensor derived RLR_{sensor}:

$$RLR_{hc\_corr}(\theta) = corr1(\theta) \cdot corr2(\theta)\, RLR_{hc} \quad (4)$$

$corr1(\theta)$ is the correction factor that normalizes the sky region area:

$$corr1(\theta) = \left[\frac{\cos(85)\cdot\sin(5)}{\cos(\theta)\cdot\sin(\Delta\theta/2)}\right], \quad (5)$$

where $\Delta\theta$ represents the resolution in elevation angle which was set to 20° in the GLA in order to parallel the 23.42° view angle of the light sensor. The $corr2(\theta)$ converts the light values to those measured from a normally incident direction:

$$corr1(\theta) = \frac{\sin(85)}{\sin(\theta)}. \quad (6)$$

Note that the zenith sector is treated as an annular piece with an average elevation angle of 85° and an angular width $\Delta\theta$ = 10°. Hence both corr1 and corr2 are equal to 1 for the zenith. Equations (5) and (6) can be derived from geometrical considerations in a straightforward manner.

As mentioned earlier, in the analyses that were completed, the RLRs were further aggregated over azimuthal angles so that they have become functions of elevation angle (θ) only, as shown.

2.7. Statistical analyses

To determine the *b* parameter, the procedure NLIN was used to fit the nonlinear regression of radiance to elevation angle using the SOC sky distribution model (Eq. (2)) under overcast days. RLR_{sensor} was subjected to a two-way analysis of variance in order to examine the effects of forest composition, elevation angle (or azimuth angle), and their interaction (no interaction was performed when the azimuth angle was used), on the angular distribution of PAR under overcast and clear sky conditions. For each analysis of variance, Tukey's test was used to compare the means. Analysis of variance was performed separately for each sky condition and time period. A four-way analysis of variance (methods, forest composition, elevation angle, and azimuth angle) was performed to test for differences between the two methods (overcast sky RLR_{sensor} and diffuse light RLR_{hc_corr}). When RLR tended to be non-normally distributed with heterogeneous variances, analyses of variance were performed on log transformed data [35, 36]. However, untransformed means and standard errors are reported in all figures. All statistical analyses were conducted using the SAS version 6.12 (SAS Institute Inc., Cary, N.C.); all of the main effects and interactions were significant to at least the 0.05 level.

3. RESULTS

3.1. Angular distribution of PAR in the open under overcast and clear sky conditions

Overcast sky RLR_{sensor} in the open decreased gradually with decreasing elevation angle under overcast skies (Fig. 1), with the maximum RLR_{sensor} occurring near the zenith at both the

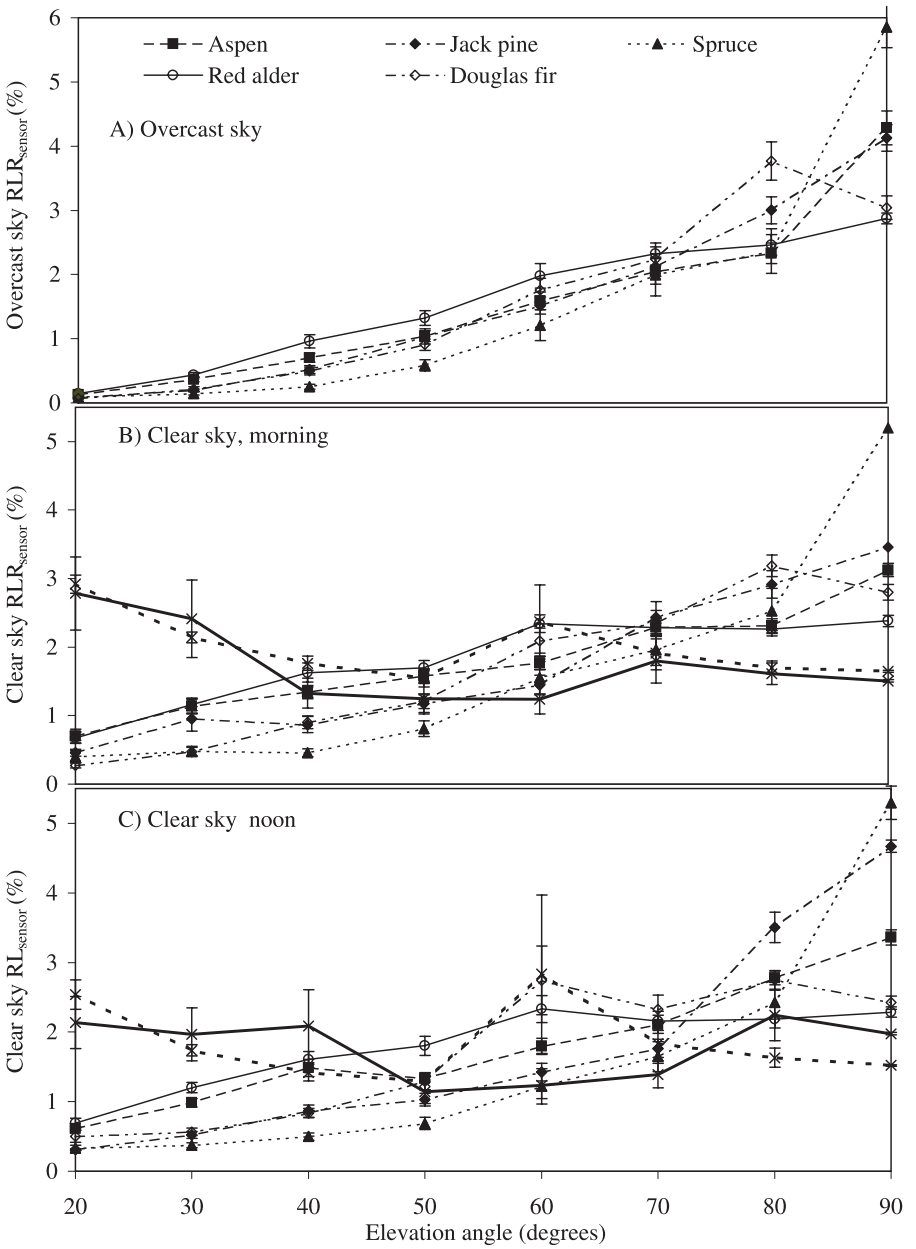

Figure 2. Relative light readings (± SE) measured with the light sensor (RLR_{sensor}) as a function of elevation angle in the aspen, Jack pine, spruce, red alder and Douglas-fir stands for (A) overcast sky, (B) clear sky in the morning, and (C) clear sky around noon. The range of solar elevation angles for the specified periods on clear days (Figs. 2B and 2C) extended from 44º to 59º and from 27º to 39º in the morning, and from 59º to 61º and from 39º to 41º around noon at the Duparquet Lake Research Station and on Vancouver Island, respectively. Relative light readings in the open on clear days are also shown by the large solid lines for the Duparquet Lake Research Station and by large dotted lines for Vancouver Island.

Duparquet Lake Research Station and on Vancouver Island. Overcast sky RLR_{sensor} in the open followed the SOC sky distribution with the zenith-to-horizon radiance ratio parameter (*b*) estimated at 3.67 (± 0.69) and 4.03 (± 2.11) at the Duparquet Lake Research Station and on Vancouver Island, respectively (Fig. 1). Clear sky RLR_{sensor} in the open consistently showed small peaks near the horizon (20° elevation) (Figs. 2B and 2C). In general, clear sky RLR_{sensor} does not exhibit any steady decrease or increase with elevation, and so it is best described with the UOC.

3.2. Effects of sky conditions and forest composition on angular distribution of PAR beneath closed forest canopies

Under both overcast and clear sky conditions, the elevation angle, the forest composition and their interactions all significantly affected RLR_{sensor} for both sites (Tab. II). Overcast and clear sky RLR_{sensor} were generally higher at the zenith and decreased almost linearly with decreasing elevation angle (Fig. 2). Although statistically different, overcast and clear sky

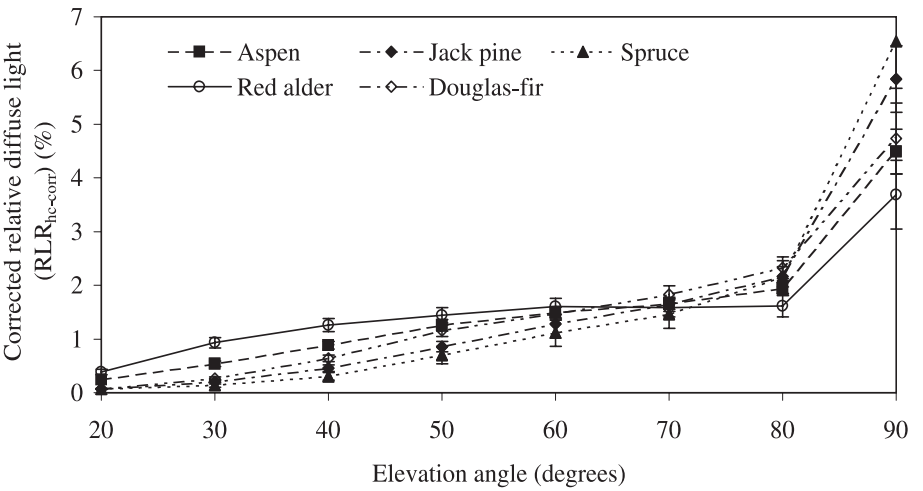

Figure 3. Corrected relative diffuse light readings (diffuse light RLR_{hc_corr}) (± SE) estimated with the hemispherical canopy photographs as a function of elevation angle in the aspen, Jack pine, spruce, red alder, and Douglas-fir stands.

Table II. ANOVA results for relative light readings in response to elevation angle and forest composition. Symbols are as follows: *** $P < 0.0001$, ** $P < 0.01$, * $P < 0.05$, NS = $P > 0.05$.

Source	Overcast sky		Clear sky, morning		Clear sky, noon	
	d_f	Mean square	d_f	Mean square	d_f	Mean square
Aspen, Jack Pine, and Spruce Stands						
Elevation angle (EA)	7	183.90***	7	64.33***	7	72.15***
Forest composition (FC)	2	22.43***	2	18.88***	2	20.11***
EA × FC	14	2.53***	14	2.85***	14	2.76***
Error	807	0.37	799	0.29	744	0.19
Red Alder and Douglas-fir Stands						
Elevation angle (EA)	7	137.79***	7	33.32***	7	29.37***
Forest composition (FC)	1	19.99***	1	17.17***	1	11.95***
EA × FC	7	4.37***	7	4.25***	7	2.44***
Error	688	0.34	564	0.22	588	0.25

RLR_{sensor} beneath aspen and Jack pine stands were qualitatively similar. Overcast and clear sky RLR_{sensor} were generally higher in the spruce stands between 90° and 80° and lower below these elevation angles, when compared to the aspen and jack pine stands. On Vancouver Island, overcast and clear sky RLR_{sensor} were generally higher in Douglas fir stands between 90° and 70º, and lower below those elevations in comparison to red alder.

The majority of RLR_{sensor} was not influenced by azimuth angles (data not shown). Overcast sky RLR_{sensor} beneath aspen, Jack pine, and spruce stands were isotropic with respect to azimuth angles for overcast skies (data not shown). Under clear sky conditions, some RLR_{sensor} were statistically higher towards the sun azimuth angles. On Vancouver Island, the majority of the RLR_{sensor} (both under overcast and clear sky conditions) was isotropic with respect to azimuth angles (data not shown). Studies of the azimuthal variation in light have not been done before so these results, while not the focus of this study, are discussed here briefly. They also provide justification for our averaging over azimuth in all other analyses in the present study.

3.3. Relative light readings estimated with the hemispherical canopy photographs (diffuse light RLR_{hc_corr}) and its comparison with overcast sky RLR_{sensor}

Diffuse light RLR_{hc_corr} was calculated in order to directly compare the angular distribution of PAR estimated with the hemispherical canopy photographs with that measured with overcast sky RLR_{sensor} (compare Fig. 2A with Fig. 3). Results showed a decrease in RLR with decreasing elevation angles,

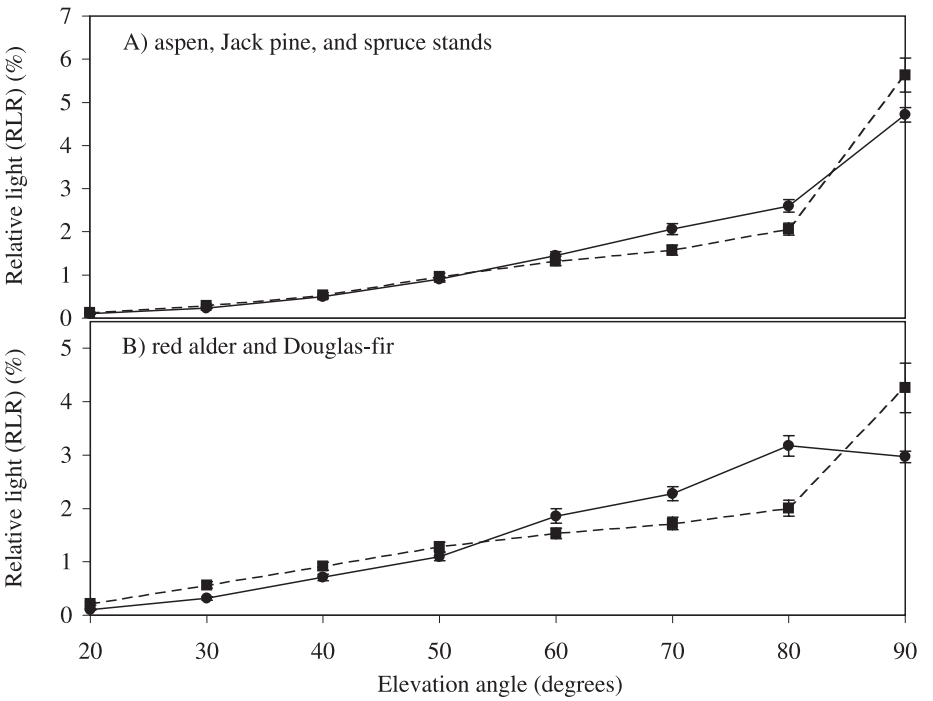

Figure 4. Comparison between the relative diffuse light readings (RLR) (± SE) measured with the sensor (solid lines: overcast sky RLR_{sensor}) and estimated with the hemispherical canopy photographs (dotted lines: diffuse light RLR_{hc_corr}) as a function of elevation angle in (A) aspen, Jack pine and spruce stands and (B) red alder and Douglas-fir stands.

Table III. Four-way ANOVA results for relative light readings under overcast skies in response to method (overcast sky RLR_{sensor} and diffuse light RLR_{hc_corr}), forest composition, elevation angle and azimuth angle. Symbols are as follows: *** $P < 0.0001$, ** $P < 0.01$, * $P < 0.05$, NS = $P > 0.05$.

Forest Stands Source	Aspen, Jack Pine, and Spruce		Red Alder and Douglas-fir	
	d_f	Mean square	d_f	Mean square
Method (M)	1	51.67*	1	14.02NS
Forest composition (FC)	2	141.25***	1	63.75**
Elevation angle (EA)	7	2483.06***	7	1261.46***
Azimuth angle (AA)	7	7.75NS	7	29.06***
M × FC	2	15.22NS	1	0.04NS
M × EA	7	15.19***	7	58.01***
M × AA	7	15.51*	7	4.50NS
M × FC × EA	28	16.63***	14	46.60***
M × FC × AA	28	27.31***	14	37.64***
M × EA × AA	98	4.43NS	98	10.12***
M × FC × EA × AA	196	3.99NS	98	5.75NS
Error	1279	5.93	1152	5.24

and also exhibited the same general trends regarding the effects of forest composition. Diffuse light RLR_{hc_corr} and overcast sky RLR_{sensor} were highest for the spruce stands above 80°, but jack pine and aspen tended to have higher RLR below 80°. On Vancouver Island, diffuse light RLR_{hc_corr} and overcast sky RLR_{sensor} were lower beneath the red alder stands compared to the Douglas-fir stands above 60°, but Douglas-fir RLR was lower below 60°. Table III, however, shows a complex set of detailed differences among the two methods, forest composition, elevation angle, and azimuth angle. These differences are reflected in the RLR graphs. For example, at both sites, the decrease in diffuse light RLR_{hc_corr} from the zenith to 80º was more pronounced than with overcast sky RLR_{sensor}, but was similar at lower elevation angles (Fig. 4).

4. DISCUSSION

4.1. Determination of the optimal zenith-horizon radiance ratio parameter (*b*) for modelling the angular distribution of diffuse PAR in the open for overcast and clear sky conditions

Few studies have characterised the PAR sky distribution on overcast days. Grace [19] reported that the SOC formula with *b* set to 2 explained nearly half of the sky variation obtained at a wavelength of 575 μm. Grant et al. [21] reported that PAR radiance was 5.6 times higher at the zenith than at the horizon, with a corresponding *b* value of 4.6. Similar to this latter study, our estimated *b* also indicates that PAR decreases more rapidly than global radiation from zenith to horizon with light at the zenith more than four times greater than at the horizon. This might result from the radiation scattering in the atmosphere being strongly wavelength selective. As radiation travels through the atmosphere, it is scattered by molecules of gas and aerosols [27]. Scattering is higher near the horizon because of the longer pathlength that the radiation travels through the atmosphere to the viewer [27]. Since the scattering is proportional to the inverse fourth power of the wavelength, the scattering of short PAR wavelengths is thus greater than the scattering of the longer wavelengths found in global radiation. This would explain the greater attenuation of PAR wavelengths compared to global radiation as the horizon is approached.

Under clear sky conditions, the angular distribution of light depends mainly on the position of the sun, and to a lesser extent on turbidity and scattering [40]. The sky sector around the sun is defined as the circumsolar region and corresponds to a peak in RLR for both global radiation [31, 32, 40] and PAR radiation [15, 21]. In the present study, however, light measurements taken when the light sensor was pointing near or at the solar elevation angles were omitted and these peaks were thus not observed. The low clear sky RLR_{sensor} measured near or at the solar elevation angles correspond to a region of low radiance in the sky hemisphere. This region, located at about 90° from the sun, shows a lower radiance than the average radiance in the sky hemisphere [40], and is about four times less bright than the circumsolar region for the PAR wavelength range [21]. Another bright region in the sky is found near the horizon. In the present study, high clear sky RLR_{sensor} measured at an elevation angle of 20° corresponds with horizon brightening as diffuse light tends to be stronger nearer the horizon than at the zenith under clear sky conditions [21, 27].

4.2. Effects of elevation angle, forest composition, and sky conditions on the angular distribution of PAR beneath forest stands

Elevation angle significantly influenced the angular distribution of PAR beneath forest stands for both overcast and clear sky conditions. Under overcast sky conditions, RLR_{sensor} beneath forest stands decreased with decreasing elevation angles. Similar patterns in diffuse light penetration were found beneath three types of forests in Japan where diffuse light penetration, calculated from photographs of canopies for various elevation angles, was observed to decrease with decreasing elevation angle [43]. The decline in RLR_{sensor} under both overcast and clear sky conditions with decreasing elevation angle is expected. Light penetration through a vegetation canopy has been shown to decline with decreasing elevation angle because light from lower angles filters through longer pathlengths in the canopy so there is increased interception by foliage, branches, and trunks [2, 3, 20]. Only a few clear sky RLR_{sensor} measurements showed significant variation with respect to azimuth angles. Most of these differences were easily explained by the location of the sun. However, since only diffuse light was measured in clear sky conditions, we would expect stronger differences in the direction of the sun when direct light is included.

Differences in the angular distribution of PAR under tree canopies could be caused by the characteristics of the forest stands. For example, in the boreal forest, aspen crowns have a spherical shape with an erectophile leaf orientation [23]. Their crowns are closely packed and form a uniform layer of leaves. Large numbers of small gaps can be seen between the leaves and the branches over the whole aspen forest canopy. This particular structure explains the penetration of lateral light, which results in a gradual attenuation of light with decreasing solar elevation angle, as measured in this study. Similarly, because of the uniform distribution of the aspen leaves, the proportion of sunflecks to radiation intensity greater than 500 $\mu mol \cdot m^{-2} \cdot s^{-1}$ was found to be lower beneath aspen stands than conifer stands in the boreal forest [26].

Overcast and clear sky RLR_{sensor} decreased sharply from the zenith to the horizon beneath the spruce stands at the Duparquet Lake Research Station. Light does not come from all directions in spruce stands since the scattering coefficient is lower for boreal spruce stands as compared with Jack pine stands [11]. Moreover, penetration of lateral light was reduced by the high crown ratio (47–69%) and the presence of long dead branches along the trunks. At high latitudes, the long conical crowns of conifers might be an adaptation to better intercept direct light at low elevation angles [24]. The interception of lateral light would result in a sharp attenuation of light coming from low elevation angles, as measured in this study. Black spruce (*Picea mariana* (Mill.) BSP), and other conifers, often have tall, narrow crowns with the majority of their shoots oriented close to the horizontal position [11]. This crown structure has been hypothesised to increase light interception at higher elevation angles [11] and thus transmit greater amounts of light at mid to low elevations. This latter hypothesis, however, is not supported by our spruce stands results, but explains the angular distribution of PAR found under our Douglas-fir stands.

The results of this study also suggest that the angular distribution of PAR beneath forest canopies varies with their specific shade tolerance. For example, RLR_{sensor} was usually higher under the shade intolerant aspen and Jack pine stands as compared to the shade tolerant spruce stands, at low elevation angles. These results are consistent with many studies that have reported that shade intolerant tree species transmit more light than shade tolerant species [9, 26]. The present study also demonstrates that shade intolerant aspen and Jack pine trees transmit light from a relatively wider angle around the zenith than shade tolerant spruce species, which transmit light mainly from the zenith.

Overcast and clear sky RLR_{sensor} were statistically higher beneath the shade intolerant red alder than Douglas-fir stands.

Above 60º–70º, however, overcast and clear sky RLR_{sensor} were similar or higher beneath the Douglas-fir stands. It has been reported in the literature that the horizontal branches of spruce and Douglas-fir trees allow greater lateral light penetration than occurs for species with a more vertical branching structure [4, 11]. As mentioned above, this was not the case in the spruce stands because the spruce stands examined in this study had very long crowns and a high live crown ratio. However, the horizontal branches in Douglas-fir trees and the low live crown ratio (less than 33%) may have permitted the penetration of lateral light at mid and high elevation angles. Mature Douglas-fir stands transmit relatively high amounts of diffuse light because they are tall, support a relatively low leaf area and have crowns that are well above the forest floor [37]. Relatively high lateral light penetration in these Douglas-fir stands would lead to smaller differences in overcast and clear sky RLR_{sensor} between the red alder stands and the Douglas-fir stands, as was observed here.

4.3. Comparison between the overcast sky RLR_{sensor} measured with the light sensor and diffuse light RLR_{hc_corr} estimated from the hemispherical canopy photographs

Two correction factors were required to properly compare RLR_{hc} with the overcast sky RLR_{sensor} (see the Methods section). With these two corrections, angular distribution of PAR estimated from hemispherical canopy photographs, diffuse light RLR_{hc_corr}, was globally in agreement with the overcast sky RLR_{sensor}. However, diffuse light RLR_{hc_corr} may blur some of the within-day variability in angular distribution of PAR since they represent azimuthally and temporally integrated values (see Methods). RLR measured with the light sensor under different sky conditions and at different periods during the day showed some variation in the angular distribution of PAR. For example, a peak in clear sky RLR_{sensor} was measured by the sensor around noon in the Douglas-fir stands (Fig. 2C). By contrast, diffuse light RLR_{hc_corr} is averaged throughout the day and the growing season by the GLA so that these temporal peaks of light were not apparent (Fig. 3). This within-day light variability is important, however, [18] as it potentially influences the physiological and morphological responses of understory plants.

5. CONCLUSION

Firstly, the angular distribution of PAR under overcast sky conditions measured with the light sensor was not found to be isotropic as modelled in some studies [7, 8]. Instead, results of this study indicate that PAR was more than four times greater at the zenith than at the horizon with a zenith-horizon radiance ratio parameter (*b*) of 3 or 4. This rapid decrease in PAR with decreasing elevation angle is concordant with Grant et al. [21] and may be attributed to multiple scattering in the PAR wavelengths near the horizon [27]. Therefore it is felt that the SOC model is a more accurate representation of the diffuse overcast sky light distribution than an isotropic, the UOC, model. Secondly, this study demonstrates that the angular distribution of PAR as described by the RLR profile under tree canopies is influenced by sky conditions, elevation angle, and forest composition. For example, aspen and Jack pine stands transmitted light from a relatively wider angle around the zenith than spruce stands, which transmitted light mainly from the zenith. Thirdly, diffuse light RLR_{hc_corr} was found to be globally in agreement with overcast sky RLR_{sensor} with regards to the effects of forest composition. However, overcast sky RLR_{sensor} showed large variations in the angular distribution of PAR under different sky conditions and periods of the day. Results of this study are useful for refining PAR models and determining the potential impact of the different angular distribution of PAR profiles in shaping crown morphology and in influencing light interception by the understory vegetation layers.

Acknowledgments: We thank Annie Morin and Joel Coburn for their help with field work, Don Carson for providing access to the Cowichan Lake Research Station and Lana B. Ruddick for editorial English comments. Funding support for this research was provided by the National Sciences and Engineering Research Council grant to F. Gendron, by the Sustainable Forest Management Network, and by Forest Renewal B.C. (Project HQ96400-RE). Support from these agencies and from the B.C. Ministry of Forests is gratefully acknowledged.

REFERENCES

[1] Ackerly D.D., Bazzaz F.A., Seedling crown orientation and interception of diffuse radiation in tropical forest gaps, Ecology 76 (1995) 1134–1146.

[2] Anderson M.C., Studies of the woodland light climate. II. Seasonal variation in the light climate, J. Ecol. 52 (1964) 643–663.

[3] Baldocchi D.D., Hutchison B.A., Matt D.R., McMillen R.T., Seasonal variations in the radiation regime within an oak-hickory forest, Agric. For. Meteorol. 33 (1984) 177–191.

[4] Black T.A., Chen J.M., Lee X., Sagar R.M., Characteristics of shortwave and longwave irradiances under a Douglas-fir forest stand, Can. J. For. Res. 21 (1991) 1020–1028.

[5] Brunger A.P., Hooper F.C., Anisotropic sky radiance model based on narrow field of view measurements of shortwave radiance, Solar Energy 51 (1993) 53–64.

[6] Canham C.D., Growth and canopy architecture of shade-tolerant trees: response to canopy gaps, Ecology 69 (1988) 786–795.

[7] Canham C.D., Coates K.D., Bartemucci P., Quaglia S., Measurement and modeling of spatially explicit variation in light transmission through interior cedar-hemlock forests of British Columbia, Can. J. For. Res. 29 (1999) 1775–1783.

[8] Canham C.D., Denslow J.S., Platt W.J., Runkle J.R., Spies T.A., White P.S., Light regimes beneath closed canopies and tree-fall gaps in temperate and tropical forests, Can. J. For. Res. 20 (1990) 620–631.

[9] Canham C.D., Finzi A.C., Pacala S.W., Burbank D.H., Causes and consequences of resource heterogeneity in forests: interspecific variation in light transmission by canopy trees, Can. J. For. Res. 24 (1994) 337–349.

[10] Chazdon R.L., Field C.B., Photographic estimation of photosynthetically active radiation: evaluation of a computerized technique, Oecologia 73 (1987) 525–532.

[11] Chen J.M., Canopy architecture and remote sensing of the fraction of photosynthetically active radiation absorbed by boreal conifer forests, IEEE Trans. Geosci. Remote Sensing 34 (1996) 1353–1367.

[12] Clarck D.A., Clarck D.B., Life history diversity of canopy and emergent trees in a neotropical rain forest, Ecol. Monogr. 62 (1992) 315–344.

[13] Clearwater M.J., Gould K.S., Leaf orientation and light interception by juvenile *Pseudopanax crassifolius* (Cunn.) C. Koch in a partially shaded forest environment, Oecologia 104 (1995) 363–371.

[14] Easter M.J., Spies T.A., Using hemispherical photography for estimating photosynthetic photon flux density under canopies and in gaps in Douglas-fir forests of the Pacific Northwest, Can. J. For. Res. 24 (1994) 2050–2058.

[15] Endler J.A., The color of light in forests and its implications, Ecol. Monogr. 63 (1993) 1–27.

[16] Fielder P., Comeau P., Construction and testing of an inexpensive PAR sensor, Res. Br., Min. For., Victoria, BC. Work.-Pap. 53/ 2000, 2000.

[17] Frazer G.W., Canham C.D., Lertzman K.P., Gap Light Analyzer (GLA): Imaging software to extract canopy structure and gap light transmission indices from true-colour fisheye photographs, users manual and program documentation, Simon Fraser University, Burnaby, British Columbia, and the Institute of Ecosystem Studies, Millbrook, New York, 1999.

[18] Gendron F., Messier C., Comeau P.G., Temporal variations in the understorey photosynthetic photon flux density of a deciduous stand: the effects of canopy development, solar elevation, and sky conditions, Agric. For. Meteorol. 106 (2001) 23–40.

[19] Grace J., The directional distribution of light in natural and controlled environment conditions, J. Appl. Ecol. 8 (1971) 155–164.

[20] Grant R.H., Ultraviolet and photosynthetically active bands: plane surface irradiance at corn canopy base, Agron. J. 83 (1991) 391–396.

[21] Grant R.H., Heisler G.M., Gao W., Photosynthetically-active radiation: sky radiance distributions under clear and overcast conditions, Agric. For. Meteorol. 82 (1996) 267–292.

[22] Hutchison B.A., Matt D.R., McMillen R.T., Effects of sky brightness distribution upon penetration of diffuse radiation through canopy gaps in a deciduous forest, Agric. Meteorol. 22 (1980) 137–147.

[23] Kucharik C.J., Norman J.M., Gower S.T., Measurements of leaf orientation, light distribution and sunlit leaf area in a boreal aspen forest, Agric. For. Meteorol. 91 (1998) 127–148.

[24] Kuuluvainen T., Tree architectures adapted to efficient light utilization: is there a basis for latitudinal gradients? Oikos 65 (1992) 275–284.

[25] Lieffers V.J., Messier C., Stadt K.J., Gendron F., Comeau P.G., Predicting and managing light in the understory of boreal forests, Can. J. For. Res. 29 (1999) 796–811.

[26] Messier C., Parent S., Bergeron Y., Effects of overstory and understory vegetation on the understory light environment in mixed boreal forests, J. Veg. Sci. 9 (1998) 511–520.

[27] Monteith J.L., Unsworth M.H., Radiation environment, in: Principles of environmental physics, 2nd ed., Edward Arnold, London, 1990, pp. 36–57.

[28] Moon P., Spencer D.E., Illumination from a non-uniform sky, Trans. Illum. Eng. Soc. 37 (1942) 707–726.

[29] O'Connell B.M., Kelty M.J., Crown architecture of understory and open-grown white pine (*Pinus strobus* L.) saplings, Tree Physiol. 14 (1994) 89–102.

[30] Reifsnyder W.E., Furnival G.M., Horowitz J.L., Spatial and temporal distribution of solar radiation beneath forest canopies, Agric. Meteorol. 9 (1971) 21–37.

[31] Rosen M.A., Hooper F.C., Brunger A.P., The characterization and modelling of the diffuse radiance distribution under partly cloudy skies, Solar Energy 43 (1989) 281–290.

[32] Ross J., The radiation regime and architecture of plant stands, Dr W. Junk Publishers, The Hague, 1981.

[33] Ross M.S., Flanagan L.B., La Roi G.H., Seasonal and successional changes in light quality and quantity in the understory of boreal forest ecosystems, Can. J. Bot. 64 (1986) 2792–2799.

[34] Rouvinen S., Kuuluvainen T., Structure and asymmetry of tree crowns in relation to local competition in a natural mature Scots pine forest, Can. J. For. Res. 27 (1997) 890–902.

[35] Scherrer B., Biostatistique, Gaëtan Morin, Canada, 1984.

[36] Sokal R.R., Rohlf F.J., Biometry. The principles and practice of statistics in biological research, 2nd ed., W.H. Freeman and Co., San Francisco, 1981.

[37] Spies T.A., Franklin J.F., Klopsch M., Canopy gaps in Douglas-fir forests of the Cascade Mountains, Can. J. For. Res. 20 (1990) 649–658.

[38] Sprugel D.G., The relationship of evergreenness, crown architecture, and leaf size, Am. Nat. 133 (1989) 465–479.

[39] Stenberg P., Simulations of the effects of shoot structure and orientation on vertical gradients in intercepted light by conifer canopies, Tree Physiol. 16 (1996) 99–108.

[40] Steven M.D., Standard distributions of clear sky radiance, Quart. J. R. Met. Soc. 103 (1977) 457–465.

[41] Steven M.D., Unsworth M.H., The angular distribution and interception of diffuse solar radiation below overcast skies, Quart. J. R. Met. Soc. 106 (1980) 57–61.

[42] Stone J.N., MacKinnon A.P.J.V., Lertzman K.P., Coarse woody debris decomposition documented over 65 years on southern Vancouver Island, Can. J. For. Res. 28 (1998) 788–793.

[43] Takenaka A., Analysis of light transmissivity of forest canopies with a telephoto method, Agric. For. Meteorol. 40 (1987) 359–369.

[44] Vales D.J., Bunnell F.L., Relationships between transmission of solar radiation and coniferous forest stand characteristics, Agric. For. Meteorol. 43 (1988) 201–223.